Wear 454-455 (2020) 203335

Contents lists available at ScienceDirect

Wear

journal homepage: www.elsevier.com/locate/wear

A study of grease lubricants under wind turbine pitch bearing conditions☆

Fabian Schwack [a,b,*], Norbert Bader [a], Johan Leckner [c], Claire Demaille [c], Gerhard Poll [a]

[a] Leibniz University Hannover, Institute of Machine Design and Tribology, DE-30167, Hanover, Germany
[b] KTH Royal Institute of Technology, Department of Machine Design, SE-10044 Stockholm, Sweden
[c] Axel Christiernsson International AB, SE-44911 Nol, Sweden

ARTICLE INFO

Keywords:
False brinelling
Wind energy
Wear
Grease
Pitch bearing
Blade bearing

ABSTRACT

Pitch bearings in wind turbines are affected by reciprocating motion due to pitch control. The combination of oscillating operation, high loads, and mixed lubrication often leads to wear. Grease lubricants in wind turbine pitch bearings should be designed to avoid such wear. Due to different available grease lubricants, the anti-wear properties are investigated under downscaled wind turbine pitch bearing conditions. The downscaling is accomplished by load simulation for a pitch bearing and analysis of the pitch movements for a 7.5 MW reference turbine. The operational conditions of the four point contact ball bearing with 5 m outer diameter are scaled to angular contact ball bearings of the size 7208. The investigations are concluded with contact model experiments. Six Industrial grease lubricants for wind turbine pitch bearings are tested that follow very different compositions. The investigations reveal, that none of the tested grease lubricants was able to reduce wear for all tested conditions. After 250 000 cycles certain conditions lead to severe wear. Therefore, the pitch controller should avoid such conditions if possible. Nevertheless, grease lubricants with low base oil viscosities and high bleeding rates are best on average for the tested conditions. Furthermore, the results of the bearing experiments are comparable to the model experiments.

1. Introduction

Reciprocating movements between rollers and raceway can lead to damage, which limits the service life. The behaviour of oscillating rolling element bearings has not been investigated in depth. Mathematical models for the fatigue life [1,2], torque [3], or film thickness [4–6] are not sufficiently validated for oscillating rolling bearings and do not produce satisfactory results [7–9]. As mechanisms, classification, and impact of resulting damage during operation are not sufficiently investigated yet, the application of rolling element bearings in oscillating applications is still coupled with high risks of premature failures and short service life.

The pitch bearing connects the hub and the rotor blade. The bearing allows the rotor blade to perform a pivoting movement around his own axis (Z_B), as shown in Fig. 1. Pitch bearings in wind turbines are subjected both to wanted oscillations, i.e., resulting from pitch control operations [10,11], and unwanted oscillations, i.e., resulting from vibrations and load variations. During standstill the wind creates micro-oscillations of the rotor blade around its axis, which are transmitted to the pitch bearing and cause micro movements of rollers relative to the bearing rings [12,13]. Due to the constant adjustment of the pitch angle during operation the pitch bearings also perform oscillating movements. A schematic representation of pitch control is shown in Fig. 1. This is done to adapt the aerodynamic angle of attack to the wind speed. The pitching of the rotor blade is used to control the power output of the turbine and to minimise loads [14]. Newer concepts further reduce loads by pitching each rotor blade individually (Individual Pitch Control) [15,16]. The used controller concept may vary according to manufacturer and local wind conditions.

In order to achieve the highest possible energy yield, the nacelle is placed high up in the air in strong wind areas (e.g. offshore) whereby a change of the lubricants can be carried out only with great time and cost expenditure. Furthermore, due to the constant rotation of the hub, the used lubricant must remain in place. Therefore, the pitch bearings in wind turbines are usually lubricated with grease.

Several publications already focused on grease composition for wear reduction of oscillating rolling element bearings [17–20]. Due to the instationary and heterogeneous operating conditions in wind turbines these results are not directly transferable. If wear occurs during oscillating operation this usually limits service life.

The main wear mechanisms occurring in oscillating rolling element bearings can be differentiated into False Brinelling and Fretting Corrosion. It should be noted that in literature several definitions of these

☆ The research was partly funded by BMWI.
* Corresponding author.
E-mail address: schwack@kth.se (F. Schwack).

https://doi.org/10.1016/j.wear.2020.203335
Received 22 December 2019; Received in revised form 1 April 2020; Accepted 30 April 2020
Available online 30 April 2020

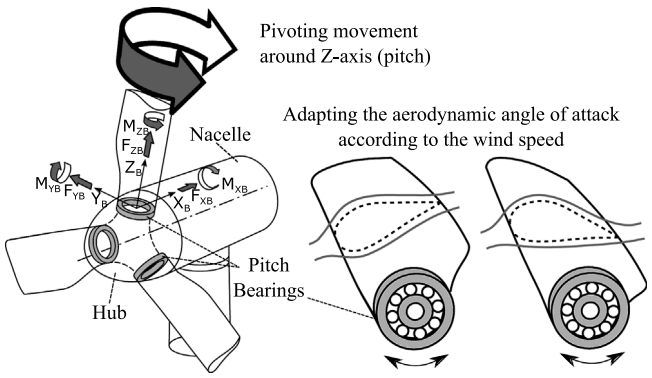

Fig. 1. Schematic representation of wind turbine pitch control.

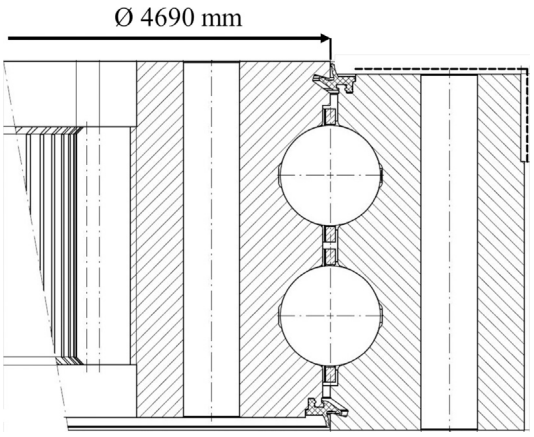

Fig. 3. Pitch bearing of reference wind turbine IWT 164-7.5-MW.

terms are in use [21]. Especially in older publications the differentiation or relationship of the mechanisms was treated inconsistently [22, 23].

False Brinelling and Fretting Corrosion can occur under similar conditions if the oscillation amplitude is so small that slip occurs in a fixed contact region. If lubricant is present False Brinelling occurs, which is characterised by three distinct areas [21], see Fig. 2(a). There is a ring-shaped area in the outer region due to pure sliding. This area surrounds a region in which partial sliding occurs. In the middle of the contact is a region where no relative movement and no wear occurs, since rolling movement between roller and raceway takes places in this region. The occurring wear is a complex mechanism that is influenced by the relative slip, the coefficient of friction, the contact pressure, and tribochemical reactions. In the outer region, the slip leads to a smoothing of the rough surface. In the region where partial slip occurs, the reaction product Magnetite is also formed because the natural oxide layer is worn away [24]. Additionally, the figure shows the movement of the roller x and the Hertz'ian contact width $2b$ [25].

The experimental results in Fig. 2(b) was obtained under the same conditions as (a) with the difference that no lubricant was used. Under dry conditions, the reaction product Hematite forms, which can be identified by its reddish colour [24]. The occurring aggressive wear is called Fretting Corrosion. This damage mechanism should be avoided, as the wear can bring particles into the system, which can lead to severe abrasive wear. False Brinelling and Fretting Corrosion both occur under oscillating conditions. Used lubricant can be squeezed out of the contact zone as the number of cycles increases. In this case, False Brinelling can escalate to Fretting Corrosion [26,27], which makes the differentiation of both terms difficult.

For big oscillating amplitudes ($x/2b>3$) Fretting mechanisms dominate if the contact partners are not separated by lubricant.

For pitch bearings in wind turbines lubricants with different properties are utilised. As pitch bearings experience varying conditions with regards to load and movement it is necessary to consider these influences when choosing a lubricant. For the presented investigations a reference turbine of 7.5 MW is analysed. All 6 tested greases are industrial products that are used in wind turbine pitch bearings. The behaviour of the lubricants is experimentally investigated using a scaled bearing test, which utilises 7208 angular contact ball bearings. To complement the bearing tests, single contact model experiments are carried out. The experimental investigations focus on the wear protection of grease lubricants that are used in wind turbine pitch bearings. The test parameters are derived by FE-simulations of the pitch bearing load during operation and analysis of the pitch bearing movements published by Stammler et al. [28].

2. Reference conditions

2.1. Reference turbine IWT-7.5-164

Generic systems are widely used in research to validate new concepts. In wind energy research generic wind turbines are an important tool as measured data can usually be attained only at high costs. In the presented work the IWT-7.5-164 (IWT) reference turbine, developed by Fraunhofer Institut for Wind Energy Systems, is used [29].

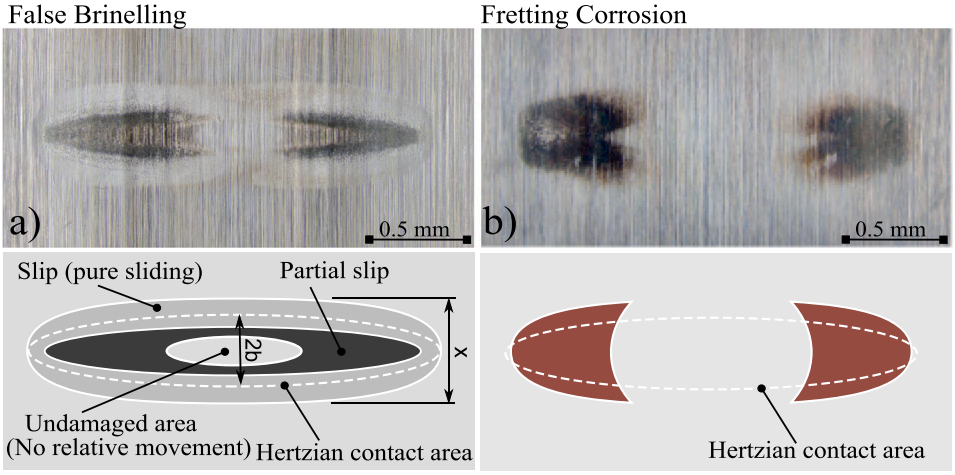

Fig. 2. Contact spot of 7208 bearing — (a) lubricated and (b) dry; $\theta = 1.0°$; $N = 25.000$ and $P = 1.9$ GPa.

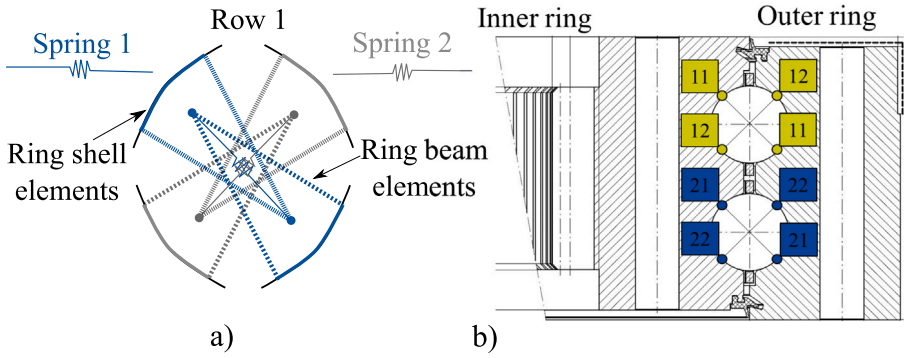

Fig. 4. (a) Simplified ball–raceway contact modelling (b) Contact labels.

Table 1
Turbine parameters.

Unit	Value
Rated power	7.542 MW
Rotor diameter	163.44 m
Specific power (per swept area)	360 W/m^2
Cut-in wind speed	3 m/s
Rated wind speed	11.7 m/s
Cut-off wind speed	25 m/s
Drive train concept	Direct Drive
Controller concept	IPC
Minimum rotational speed	5 rpm
Rated rotational speed	10 rpm
Hub height	120 m
Rotor blade length	79.98 m
Tip-speed ratio	7.31

Other reference wind turbines were developed by National Renewable Energy Laboratory (5 MW) [30] and Technical University of Denmark (10 MW) [31]. The IWT is a direct drive three blade turbine with load optimised control concept and blade design [29]. The turbine is designed for wind class IEC A1 [32]. The main parameters are given in Table 1.

The rated power output of 7.5 MW is reached at 11.7 m/s wind speed. At this speed the maximum thrust force of 1075 kN occurs. To control the power output and loads, pitching starts at 11.7 m/s.

2.2. Reference pitch bearings

The pitch bearing of the IWT is a two row four point contact bearing with a rolling diameter of 4 690 mm, outer diameter of 5 000 mm, a ball diameter of 80 mm, and 147 rollers per row. The gear for the pitch drive is on the inside of the bearing. Therefore, the inner ring is connected to the pitch bearing and the outer ring to the rotor hub. A detailed description can be found in [33]. A cross section is shown in Fig. 3.

3. Operating conditions

3.1. Loads

Analysis of the bearing behaviour necessitates the knowledge of the load distributions in the bearing. The combination of high stresses and micro oscillations usually causes severe wear [34].

Chen et al. [35] investigated the load distribution in four point contact pitch bearings of a 1.5 MW turbine with Finite Element Method (FEM). Stammler et al. [36] investigated three row cylindrical roller bearings of a 3 MW turbine. Further publications concerned with the load distribution in pitch bearings are by Becker [37] or Wang et al. [38]. Furthermore, numerous publications exist which are concerned with the load distribution in slewing bearings. Work concerning the loads

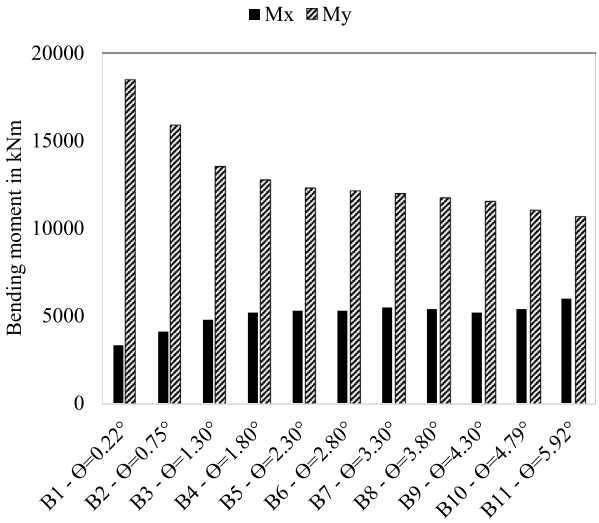

Fig. 5. Occurring loads during operational conditions.

in four point contact bearings are also relevant for the analysis of pitch bearings. Liu et al. compared their simulation results to experiments [39]. Massi et al. investigated the contact behaviour of slewing bearings [40,41]. Aguirrebeitia et al. investigated the load-carrying capacity for slewing bearings [42–45]. Special focus can be put onto the work by Daidie et al. [46] who uses non-linear springs to represent the rollers. The model used in this paper is based on the work by Daidie et al. [46] and does not take the surrounding stiffness into account, since the maximum pressure will be used for the scaling process. A schematic representation of the Daidie-approach for four point contact ball bearings is given in Fig. 4(a).

A total of 11 load cases from Schwack et al. [33] were simulated. The load cases are dependent on the pitch activity and the association of load and pitch movement is accomplished via Range-Pair-Counting as presented by Stammler et al. [28]. The coordinate system is given in Fig. 1 and the naming of the contacts of inner and outer raceway are shown in Fig. 4(b). The dominating bending moments M_x and M_y are presented in Fig. 5 together with the mean double oscillation amplitude $\hat{\theta}$ for the respective load case. The values in Fig. 5 are the maximum values determined during the simulation. For B1 the maximum bending moment M_x is 3 306 kNm and M_y reaches 18 488 kNm. For B11 M_x is higher with 5 965 kNm. The M_y bending moment reaches 12 240 kNm.

As no extreme load cases are simulated the load distributions are similar to each other. Thus, the cases maximum load and minimum oscillating amplitude (B1) (Figs. 6–8) and minimum load and maximum oscillating amplitude (B11) (Figs. 9–11) are presented. For a better

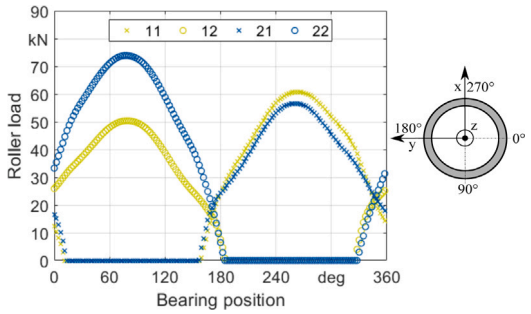

Fig. 6. Roller load during operating condition B1.

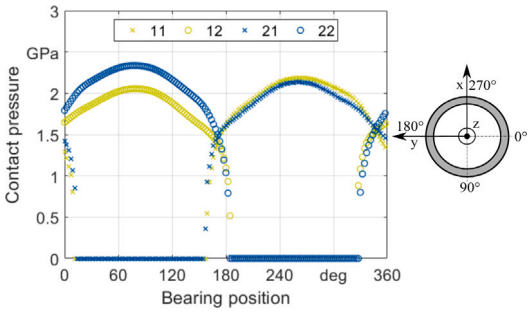

Fig. 7. Contact pressure during operating condition B1.

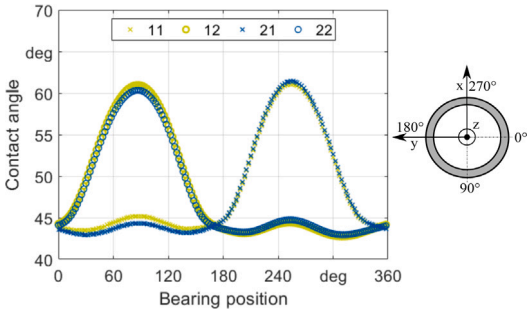

Fig. 8. Contact angle during operating condition B1.

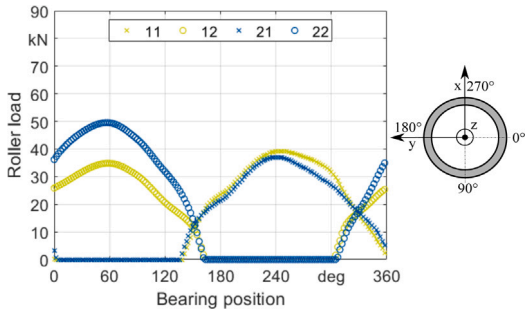

Fig. 9. Roller load during operating condition B11.

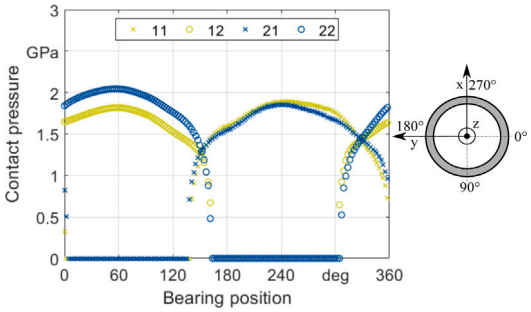

Fig. 10. Contact pressure during operating condition B11.

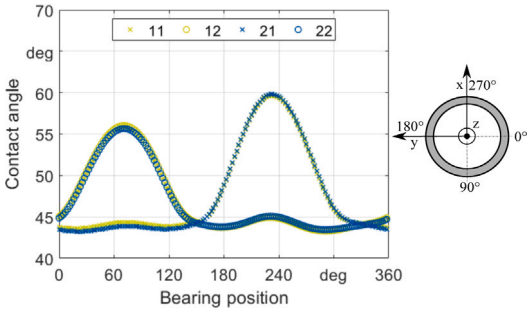

Fig. 11. Contact angle during operating condition B11.

overview the used coordinate system for the pitch bearing and the circumferential bearing position is given for each Figure.

Analysis of the bending moments M_x and M_y show that M_x increases with increased $\hat{\theta}$ while M_y decreases and that M_y is higher than M_x. For load case B1 the highest contact loads of 70 kN are reached. This occurs at around 90° and position 22. The maximum loads for the second row occur offset by 180°. These contact loads lead to a Hertz'ian pressure of 2.4 GPa. Due to the roller loads the nominal contact angle of 45° increases up to 60°. Nevertheless, truncation does not occur. For load case B11 the maximum contact load is 50 kN occurring at 60° and leads to Hertz'ian pressures of 2 GPa. The load analysis gives detailed information on occurring load situation during operational conditions and can be used as input data for the experiments.

3.2. Bearing kinematics

The oscillating movement is the main reason for increased wear in pitch bearings. The oscillation is mainly caused by the pitch controller. To understand the oscillating amplitudes and occurrence frequency of respective amplitudes the IWT pitch movements are analysed.

Using a counting method described by Stammler et al. [28] the oscillating behaviour can be deduced. First an amplitude range θ_r is defined. The IWT data was analysed in 0.2° steps, such that, e. g., if the oscillation is between 0.2 and 0.4° the number of cycles N is increased by +1 for the step $i = 1$. Additionally the real oscillating angle θ is saved so that at the end of the analysis the mean angle $\hat{\theta}_{i=1}$ can be determined. The same method is applied for frequency f_i and load P_i. The analysis was accomplished for a turbine life of 20 years.

A total of $56{\cdot}10^6$ pitch cycles were analysed by Stammler et al. revealing that small pitch amplitudes occur more often [28]. The analysis considers all cycles that occur over 20 years during the pitch controller is active. A number of $8.66{\cdot}10^6$, i. e., 15.3%, of all pitch movements occur between of 0.03 and 0.2°. The scaling will be accomplished with the data of Stammler et al. and a constant contact pressure of 1.9 GPa.

3.3. Scaling

Scaling of the loads and kinematics is based on pressure and movement distance x in relation to the Hertz'ian half width $2b$ [25]. It is assumed that the loaded surface area determines the wear. To keep the area to cycle ratio constant in different physical dimensions, the ratio of swept area to contact area is kept constant for all sizes. This furthermore, leads to identical contact kinematics. This means that for a smaller bearing the scaled oscillating angle increases in comparison

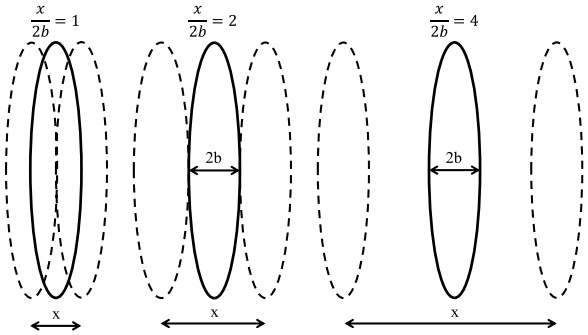

Fig. 12. $x/2b$-ratio.

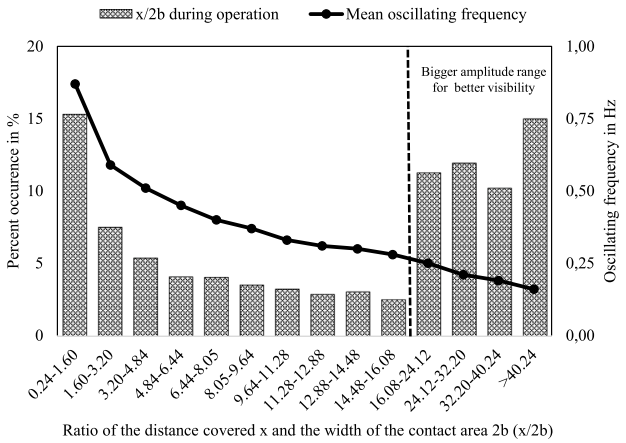

Fig. 13. Pitch behaviour of IWT-7.5-MW.

to a larger bearing. This leads to similar wear marks in scaled bearings when compared to wear from large bearings [47].

Fig. 12 shows different $x/2b$ ratios. The ellipse in the centre shows the Hertz'ian contact ellipse and the dashed lines the movement distance.

For scaling, the $x/2b$ ratio is kept constant for both bearing sizes. As scaling is possible both from big to small as well as from small to big, the superscript I is used for input data and O is used for output.

$$\frac{x^O}{2b^O} = \frac{x^I}{2b^I} \tag{1}$$

First the contact point between roller and raceway $D_{P,O}$ needs to be found from the rolling diameter D_P, roller diameter D_{WK}, and contact angle α.

$$D^I_{P,O} = D^I_P + D^I_{WK}\cos(\alpha^I) \tag{2}$$

$$D^O_{P,O} = D^O_P + D^O_{WK}\cos(\alpha^O) \tag{3}$$

With the known data of both input and output the values A_h, B_h, and τ can be calculated according to Hertz'ian theory [25].

$$b = \nu_{Hertz}\sqrt[3]{\frac{3Q(1-2\sigma^2)}{E\sum\rho}} \tag{4}$$

In the presented case b can be determined as:

$$b = \nu_{Hertz}\sqrt[3]{\frac{3F_N V}{2(A+B)}} \tag{5}$$

Using the formula of Hertz the maximum pressure P_{max} can be calculated.

$$p_{max} = \frac{3F^I_N}{2\pi ab} \tag{6}$$

Additionally the maximum roller speed v_{max} is used to determine the scaled oscillating frequency f.

$$v^I_{max} = \pi x^I f^I \tag{7}$$

Since most operational conditions of the pitch bearing leads to boundary or mixed lubrication, the roller velocity is set as constant for Input and Output for scaling:

$$v^I_{max} = v^O_{max} \tag{8}$$

A few conditions with large oscillating amplitudes can lead to hydrodynamic lubrication with a minimum film thickness h_{min}. For example a turbine which makes use of pitch control for an emergency stop of the turbine. For this rare conditions the lambda ratio Λ should be set constant. Since these operating conditions are rare and the establishment of a lubricant film depends on the used grease lubricant, we choose to keep v_{max} constant. This is a conservative approach, which leads to harsher conditions in the scaled bearing.

$$\Lambda^I = \Lambda^O \tag{9}$$

$$\Lambda = \frac{h_{min}}{\sqrt{R^2_{a1} + R^2_{a2}}} \tag{10}$$

Additionally the Hertz'ian pressure is kept identical:

$$p^I_{max} = p^O_{max} \tag{11}$$

Thus the contact normal force F_N can be determined:

$$F^O_N = \left(\frac{2}{3}\pi\mu^O_H v^O_H P^O_{max}\right)^3\left(\frac{3V}{2(A^O_h + B^O_h)}\right) \tag{12}$$

With F^O_N the contact half width b^O can be calculated:

$$b^O = v^O_H\sqrt[3]{\frac{3F^O_N V}{2(A^O_h + B^O_h)}} \tag{13}$$

And from the half width b^O the thrust load F_{Ax} for the scaled bearing (in this case type 7208) can be estimated as:

$$F^O_{Ax} = F^O_N n^O_B \sin(\alpha^O) \tag{14}$$

The presented method allows scaling of loads and movements between arbitrary bearing sizes. Fig. 13 shows the $x/2b$-ratios for the reference pitch bearing if the analyses of load situation and contact kinematics are considered. The movement data were taken from Stammler et al. [28] in which large oscillating angles were divided in larger classes. This is shown with the dashed line in Fig. 13. Due to the results shown in Fig. 13 the experiments focus on two $x/2b$ ratios:

- The region below 1.6. $x/2b$<1.6 occurs 15.3% of the time the turbine is active.
- The area from $x/2b$=10 to 15.

4. Lubricants

The lubricants in widespread use in pitch bearings are greases. In the experiments 6 lubricants commonly used in pitch bearing applications are investigated. Table 2 gives the main properties of the greases. It is apparent that there are significant differences between the greases, i. e., different base oil types, base oil viscosities between 13 and 420 mm^2/s, different thickener types, NLGI classes from 1 to 2 are compared. The lack of a red line in the grease compilation shows the complexity of grease lubricants for wind turbine pitch bearings. Greases are comprised of a base oil, which is lubricating the contact, and a thickener to increase the consistency. Commonly used thickeners

can be metal soaps, e. g., Lithium (Li), Calcium (Ca), complex, e. g., Lithium Complex (LiX), Calcium Complex (CaX), or non-soap like with Polyurea [48]. Currently the Li, LiX, Ca, CaX form the majority of greases in applications and thus also the main focus of the investigation.

The base oils can be Mineral, Synthetic, or Ester oils with added additives. The contacts are lubricated by the base oil bleeding from the thickener. The forces keeping the base oil in the thickener structure are mainly VAN-DER-WAALS and capillary forces. A higher concentration of thickener will lead to a higher consistency of the grease.

One of the mechanisms widely used to explain the lubrication of greases is, that the grease is distributed by the moving parts in the bearing and thus situated adjacent to the race tracks. From this grease oil bleeds out and flows, driven mainly by surface tension, to the contacts. This oil then lubricates the contacts. Due to this mechanism, grease lubricated systems usually run in a regime with very little oil present. This in itself is not negative as it may lead to light starvation, which can cause low friction losses due to the absence of excessive churning. In the case of oscillating applications this however may pose a big challenge.

Thus, the choice of the base oil, thickener and viscosity behaviour greatly depends on the application. In the case of wind turbine pitch bearings the following points need to be considered:

- Temperature encountered in the bearings ranging from low to moderate, with the low temperature range posing the greatest challenges for a reflow of the grease.
- During rotation of the hub and vibrations the grease needs to stay in place to allow the bleed oil to replenish the contacts.
- The replenishment should be ensured in a stable manner over the operating life of the turbine and across all operating conditions. This means a high oil content is favourable, and the base oil should be bleeding at a constant rate from the thickener.

As some of the requirements are contradicting, the choice of grease is always a compromise. A too high consistency for example may lead to the grease not changing its position during operation, however, also restricts the oil bleed. The choice of a low viscosity base oil leads to high mobility of the oil, i. e., the contacts are resupplied easily, however, the base oil can also flow away and be lost for replenishment.

The lubricants contain additives and solid lubricants, which may influence the wear behaviour. Since the focus of the work is the comparison of industrial grease lubricants, which are used in pitch bearing of wind turbines, the chemical composition of the greases is not fully known.

MARUYAMA ET AL. conducted oscillating tests with bearings of the size 51305 with different grease lubricants [49]. The $x/2b$-ratio was varied between 0.6 and 2.0, using a maximum contact pressure of 3.24 GPa. 14 greases with Urea thickener, Poly-α-olefin oil and base oil viscosities between 19 and 396 mm^2/s at 40 °C were tested. Also the influence of the worked penetration was investigated. MARUYAMA ET AL. concludes that wear can be reduced for $x/2b > 1$ by increasing the oil separation. This can be accomplished by decreasing the viscosity or increasing the worked penetration. The results are explained by the fact that the bleed oil is removed from the contact area and a thickener layer forms that reduces wear. Furthermore, it is concluded, that low viscosity base oils show good performance at high velocities, while high viscosity base oil show good performance at low velocities.

5. Experiment

5.1. Scaled bearing experiment

From the operating conditions and the scaling method the conditions for the experiments can be deduced. The bearing experiments are conducted using 7208 angular contact ball bearings as the contact mechanics are comparable to axial loaded four point contact bearings. The dimensions of the 7208 bearings are given in Table 3.

Table 2
Overview of grease properties.

Grease	Base oil	NLGI	Thickener	Base oil viscosity[a]
1	Syn.	2	Li	50 mm^2/s
2	Ester	2	Li	295 mm^2/s
3	Syn.	1–2	LiX.	420 mm^2/s
4.	Min./Syn.	1–2	Ca	13 mm^2/s
5	Min./Syn.	2	CaCx	134 mm^2/s
6	Min./Syn.	1	LiX	130 mm^2/s

[a]Measured at 40 °C.

Table 3
Bearing geometry.

Outer diameter D	80 mm	
Inner diameter d	40 mm	
Contact angle α	40°	
	OR	**IR**
Osculation	93.8%	96%

Table 4
Test conditions.

$x/2b$	Frequency f	Cycles N
0.9	8 Hz	250 000
13.3	2.3 Hz	250 000

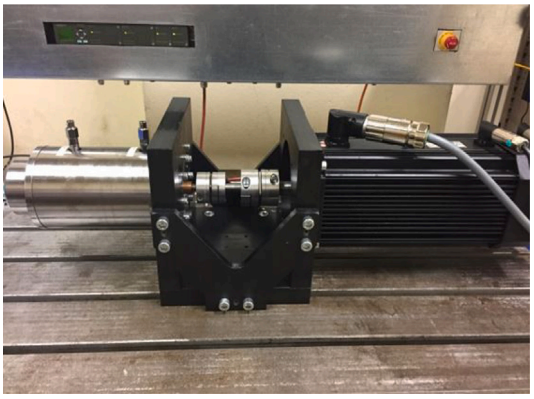

Fig. 14. Test rig.

The test rig shown in Fig. 14 consist of an electrical drive, which oscillates the shaft on which the tested bearings are mounted. The electrical drive allows high accelerations and can vary oscillating amplitudes precisely due to the control. Drive and shaft are connected via a torsionally stiff clutch. Fig. 15 shows a cutaway of the design with the face-to-face mounted test bearings. A thrust load of up to 40 kN can be applied via disc springs in different configurations.

The operating parameters are given in Table 4. $x/2b$=0.9 represent small oscillation amplitudes with relatively high frequencies and $x/2b$=13.3 represent pitch amplitudes due to wind changes. Both test conditions will run 250 000 cycles at 20 °C. All bearings are cleaned in white spirit at 60 °C for 15 min. During this cleaning step the bearings are in motion from time to time. The bearings are then rinsed, while rotating the bearing, with Isopropanol in order to remove all residues of the corrosion protection. In the last step, the bearings are heated to 80 °C for 15 min so that any residues of the Petroleum and Isopropanol evaporate. Similar to wind turbine pitch bearings, 60% of the swept volume are filled with grease. Before each test the bearings are subjected to 3 full rotations under load to distribute the grease.

5.2. Evaluation of tests

To quantify the surface changes the damage ratio as introduced by MARUYAMA ET AL. is used [9,49]. It is the ratio of the surface roughness

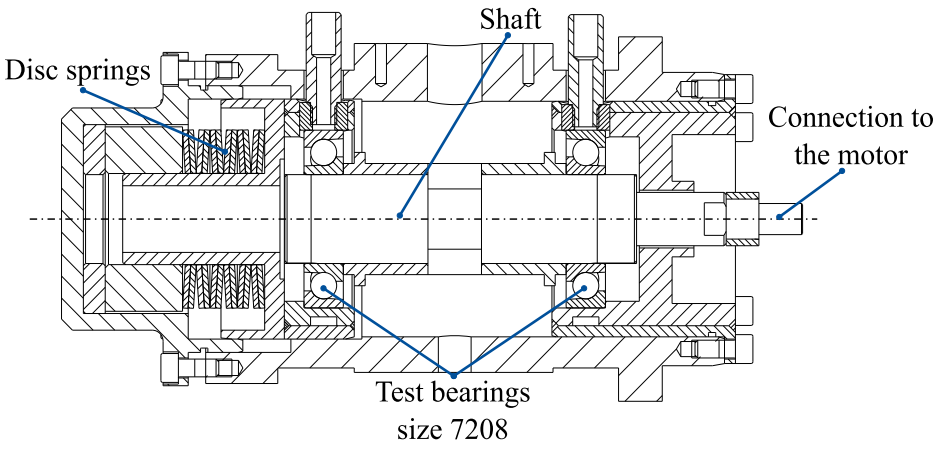

Fig. 15. Sectional view of test rig.

Table 5
Test conditions SRV.

	SRV1	SRV2
Test time	2 h	8 h
Oscillating frequency	32 Hz	8 Hz
Normal load	100 N	
Max. pressure	2.2 GPa	
Sliding distance	0.3 mm	
$x/2b$	1	
Ball Diameter	10 mm	
Ball Material	ANSI 52100	
Bed Material	ANSI 52100	

after Sz_{EXP} to before Sz_{NEW} the experiment. The results show the mean damage ratio and standard deviations across the contact points of the inner ring in one test bearing. Furthermore, optical investigations of the wear marks are performed using a laser scanning microscope.

$$SG = \frac{Sz_{EXP}}{Sz_{NEW}} \tag{15}$$

5.3. Model test (pure sliding)

In addition to the scaled bearing experiments a model setup was also utilised. The model experiments were done on a **S**chwingungs–**R**eib**v**erschleiß(SRV) tester and defined in the standard DIN 51834 [50]. Here a test specimen (i. e., ball), loaded with a defined force of 100 N, is moved with linear reciprocating motion on a steel plate. The test is widely used to investigate grease life and efficiency.

Two parameter sets following a high oscillating frequency of 32 Hz and $x/2b$=1 for N=230 400 (2 h) and low frequency of 8 Hz and $x/2b$=1 for N=230 400 (8 h). The normal force of 100 N results in 2.2 GPa Hertz'ian pressure. The experiments were accomplished at 20 °C. Each grease was tested 3 times for each test conditions. The evaluation of the wear is done by measuring the diameter of the wear mark on the ball. A microscopical image is shown as an example in Fig. 16. The result shows the mean diameter and standard deviations of 3 experiments. It must be pointed out, that the SRV contact operates under pure sliding, while the bearing operates under a rolling–sliding motion. Thus, a direct comparison of the results is not possible. However, an idea of the grease behaviour in contacts with high slip may be attempted. The parameters for the SRV tests are given in Table 5.

5.4. Grease analyses

Before and after the scaled bearing tests, the properties of the grease lubricants are analysed. The bleeding rate before the tests are determined according to DIN 51817 [51]. The NLGI class is measured according to DIN ISO 2137 [52]. It should be noted that wear particles are not removed after the experiments and thereby influence the measured NGLI class after the experiments. Furthermore, the content of wear particles and contaminations are measured according to ASTM D6595-17 [53].

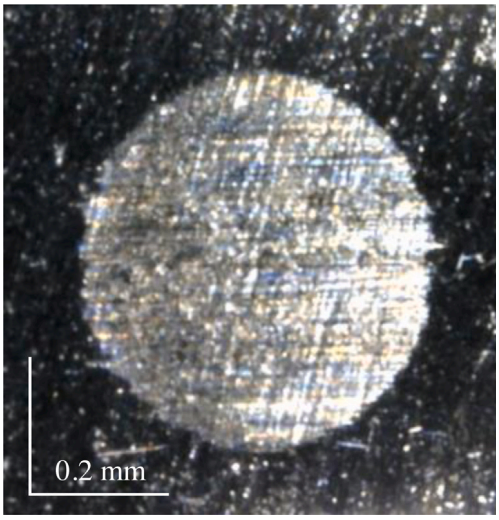

Fig. 16. Microscopy of a wear mark on ball – SRV 1 – Grease 2.

6. Results

In the following section we present the results for the investigated greases. For the bearing experiments 14 contacts are shown as photos for the $x/2b$=0.9 and $x/2b$=13.3 tests. The SRV results are shown in a tabular form. Furthermore, bearing experiments with $x/2b$=29.1 were accomplished in which no wear was detectable. Thus these results are omitted in the further discussion.

6.1. Grease 1(reference)

The results of the $x/2b$=0.9 experiments are shown in Fig. 17. For $x/2b$=0.9 only the upper half of the damaged area is shown. For the used angular contact ball bearing this area will show the highest amount of wear due to the superposition of spin and Heathcote-slip [54, 55]. Only mild wear is distinguishable in a very narrow area. The colour of the modified surface points to Magnetite. Hematite cannot be optically identified. This is an indication, that the transition to fully dry conditions and thus harsh Fretting Corrosion has not occurred yet. The

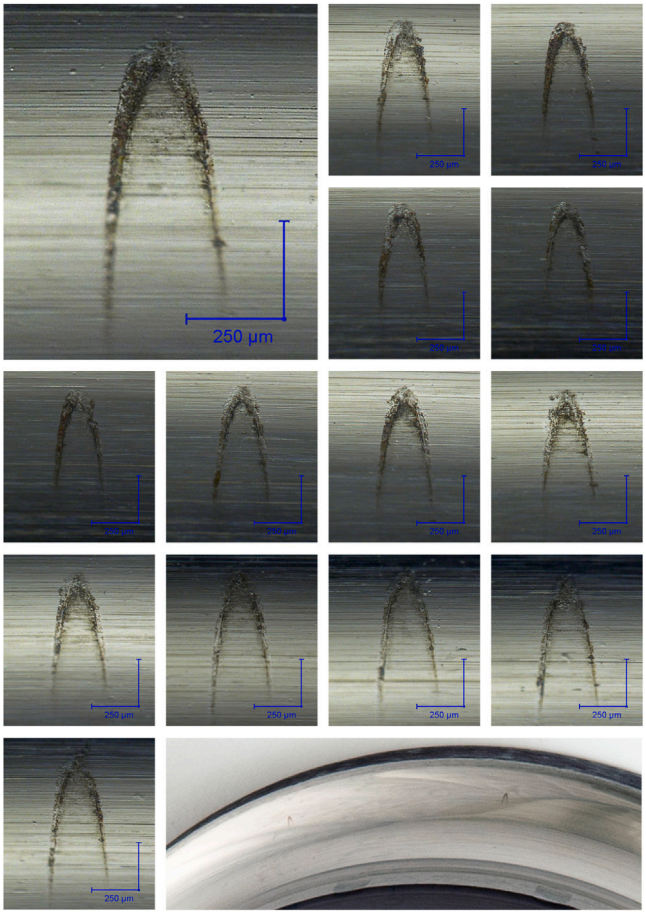

Fig. 17. Surface microscopy – $x/2b$=0.9 – Grease 1.

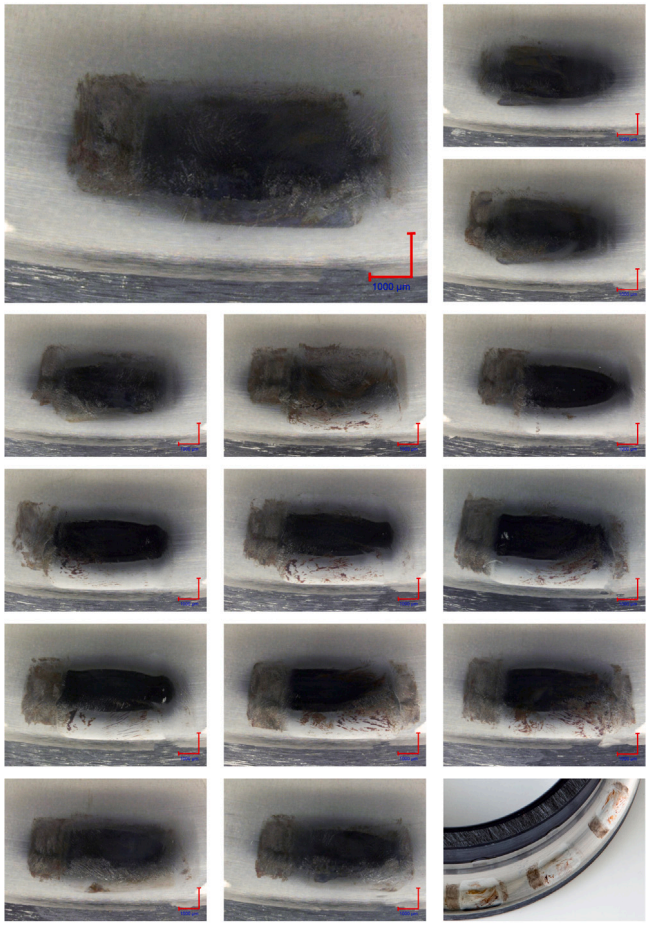

Fig. 18. Surface microscopy – $x/2b$=13.3 – Grease 1.

damage ratio was determined to be 3.16 ± 0.7. Analysis of the lubricant after experiment shows a slightly raised content of Iron (40 mg/kg) and Silicon (93 mg/kg) in comparison to an unused sample (Iron 27 mg/kg, Silicon 24 mg/kg). The consistency of the grease was unchanged by the experiment.

Fig. 18 shows the wear marks from the $x/2b$=13.3 experiments. The wear marks show a presence of Hematite especially in the reversal points, indicating a metal to metal contact. In the majority of the wear marks the centre looks polished, which points out to wear debris in the contact. Three marks also show Hematite. All marks show that the original surface profile has been changed. Furthermore, isolated pittings can be found. The grease analysis supports the observation of more severe wear as 19605 mg/kg Iron, 196 mg/kg Chromium, and 122 mg/kg Manganese was found. The consistency of the grease was only slightly changed. The damage ratio is determined as 4.55 ± 0.52, however, it needs to be noted that a polishing of the surface due to asperity contacts will yield a smoother surface after the experiment. Thus, the damage ratio is limited in its use to describe the full wear situation.

After the SRV-test the diameter of the wear scar is measured. For SRV 1 the wear scar diameter was 0.33 ± 0.006 mm. For SRV 2 a diameter of 0.35 ± 0.010 mm occured.

The grease was specifically developed for oscillating applications. It has a base oil viscosity of 50 mm^2/s at 40 °C and an oil bleed rate of 4.4%. For small $x/2b$ ratios the lubricant could limit the wear compared to other greases. With higher $x/2b$ ratios, harsh wear was observed.

Due to the solid lubricant particles in the grease and the low base oil viscosity the grease seems suitable for low $x/2b$ ratios. Table 6 shows the summary of the results.

Table 6
Summary — Grease 1.

Base oil viscosity at 40 °C	50 mm^2/s
Thickener	Lithium
Base oil	Synthetic
Measured oil bleeding (168 h) at 40° C	4.4%
Damage ratio x/2b=0.9	3.16 ± 0.7
Damage ratio x/2b=13.3	4.55 ± 0.5
Iron content fresh grease	27 mg/kg
Iron content after x/2b=0.9	41 mg/kg
Iron content after x/2b=13.3	19 605 mg/kg
NLGI fresh grease	2
NLGI after x/2b=0.9	2
NLGI after x/2b=13.3	2
Wear SRV1	0.33 ± 0.006 mm
Wear SRV2	0.35 ± 0.010 mm

6.2. Grease 2

For Grease 2 the $x/2b$=0.9 experiments False-Brinelling marks were clearly visible, see Fig. 19. The three demarcated areas defined by Grebe for False-Brinelling are clearly identifiable [56]. In the upper part of the wear mark changes of the surface are visible. The damage ratio was determined as 3.56 ± 1.59. Additionally indications of corrosion are visible, which might be related to particles.

The $x/2b$=13.3 experiments in Fig. 20 show harsh wear in all areas of the wear marks with clear indications of Hematite. This indicates dry contact. Furthermore, isolated pittings were found. The damage ratio was determined as 6.01 ± 4.48.

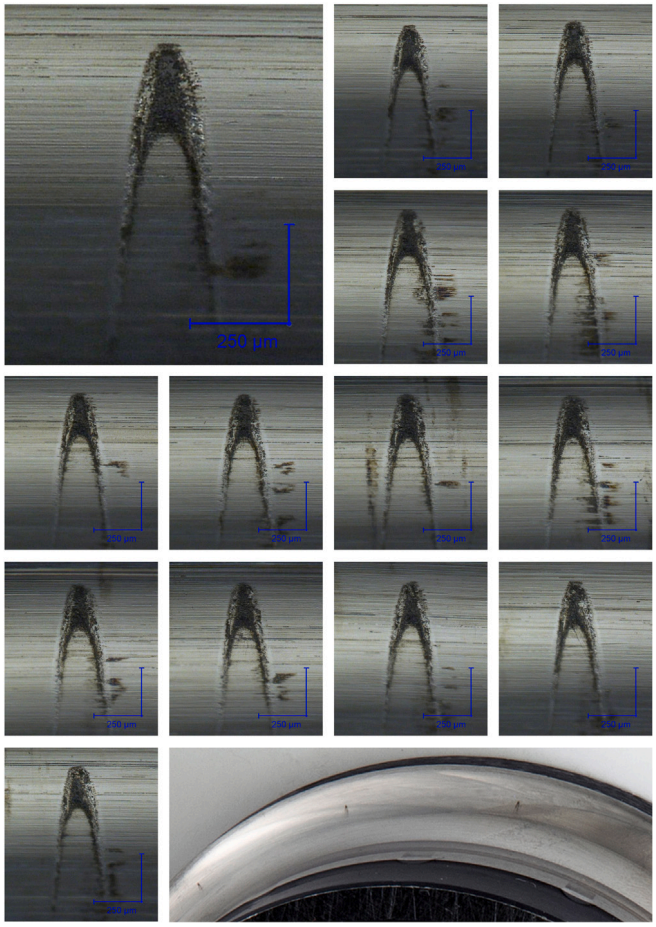

Fig. 19. Surface microscopy – $x/2b$=0.9 – Grease 2.

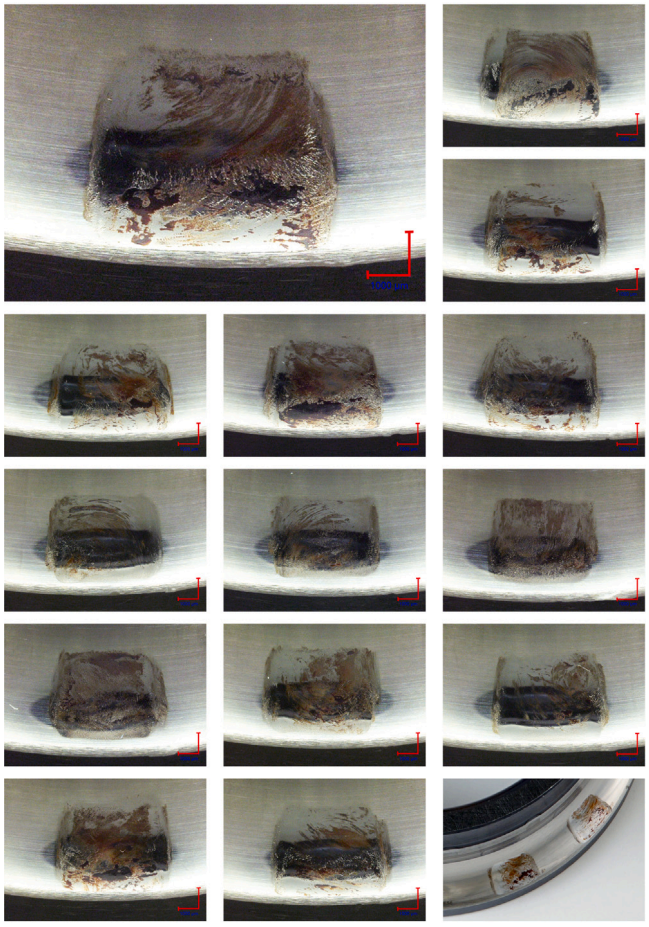

Fig. 20. Surface microscopy – $x/2b$=13.3 – Grease 2.

Table 7
Summary — Grease 2.

Base oil viscosity at 40 °C	295 mm²/s
Thickener	Lithium
Base oil	Ester
Measured oil bleed (168 h) at 40 °C	2.2%
Damage ratio x/2b=0.9	3.56 ± 1.59
Damage ratio x/2b=13.3	6.01 ± 4.48
Wear SRV1	0.56 ± 0.020 mm
Wear SRV2	0.48 ± 0.008 mm

For SRV 1 the wear scar diameter is 0.56 ± 0.020 mm. For SRV 2 the diameter of the wear scar is 0.48 ± 0.008 mm.

Grease 2 shows more wear than Grease 1 both in the $x/2b$=0.9 and x/2b=13.3 experiments and the SRV tests 1 and 2. It is assumed that the high base oil viscosity of Grease 2 leads to worse re-flow of the base oil into the contact. This is aligned with observations by Maruyama [49]. All results can be seen in Table 7.

6.3. Grease 5

For Grease 5 the form of the wear marks of the $x/2b$=0.9 experiments is similar to the wear marks found with Grease 1, see Fig. 21. Here the wear marks are also very narrow. The typical three slip zones as described by Grebe [56] are very close to each other. In the upper half, where the spin and longitudinal slip are superimposed in the same direction, changes of the surface and adhesive areas are clearly visible. The analysis of the grease shows a rise of the Iron content from 50 mg/kg compared to 15 mg/kg in the fresh grease. The consistency is slightly changed as well (NLGI class decrease from 2 to 1.5 after experiment. The measured damage ratio is 4.37 ± 1.21.

The $x/2b$=13.3 experiments show both wear marks with harsh wear and marks with nearly no visible wear, see Fig. 22. The Iron content in the lubricant (mean between several wear marks) is 11 017 mg/kg and the consistency is very low reaching a NLGI class of only 0.5. The measured surface roughness leads to a damage ratio of 3.96 ± 1.79.

The results of SRV 1 shows 0.33 ± 0.016 mm wear and 0.32 ± 0.032 mm for SRV 2. A comparison with the mean values from bearing experiments is difficult due to the different results for each contact spot.

Grease 5 showed wear for small $x/2b$ ratios in small areas. However, in these small areas the wear was very pronounced. For $x/2b$=13.3 experiments wear was partly prevented. The wear marks found clearly show a dependency on the position in the bearing. Areas that are situated at the top of the bearing are more damaged than the ones at the bottom due to the grease distribution caused by gravity. The consistency decreased during the experiments further enhancing this effect. The decreased consistency after the experiments indicates that the thickener was damaged by the stress of the test conditions. Additionally, the oil bleed rate after the test were measured and compared with the oil bleed rate before the tests. The filter paper method was used for this. A certain amount of grease is heated to 60 °C for 2 h. The diameter of the oil stain is measured. The occurring measured values before and after the experiments can be set in relation to make a statement on changing oil bleed rate. After the $x/2b$=0.9 experiment

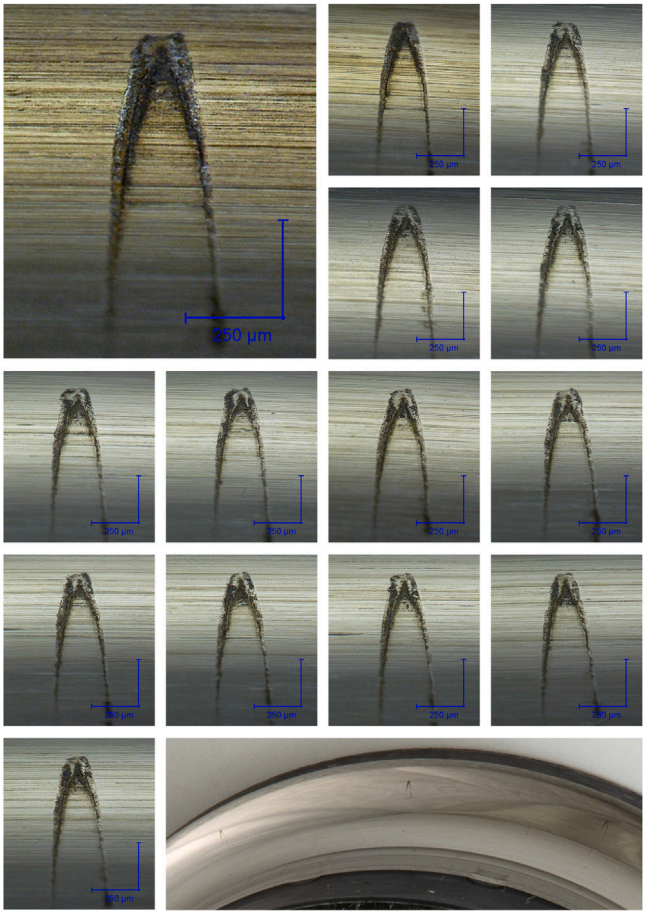

Fig. 21. Surface microscopy – $x/2b$=0.9 – Grease 5.

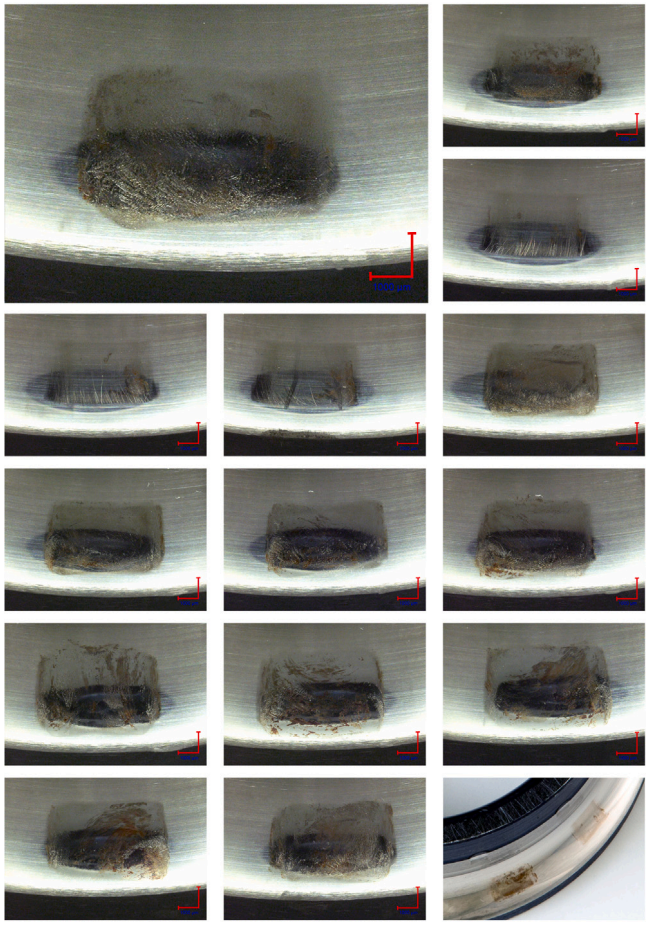

Fig. 22. Surface microscopy – $x/2b$=13.3 – Grease 5.

Table 8
Summary — Grease 5.

Base oil viscosity at 40 °C	134 mm^2/s
Thickener	Calcium-Complex
base oil	Mineral/Synthetic
Measured oil bleeding (168 h) at 40 °C	1.6%
Damage ratio x/2b=0.9	4.37 ± 1.21
Damage ratio x/2b=13.3	3.96 ± 1.79
Iron content fresh grease	15 mg/kg
Iron content after x/2b=0.9	59 mg/kg
Iron content after x/2b=13.3	11 017 mg/kg
NLGI fresh grease	2
NLGI after α	1.5
NLGI after β	0.5
Wear SRV 1	0.33 ± 0.016 mm
Wear SRV 2	0.32 ± 0.032 mm

the oil bleed rate was 51.5% higher compared to the oil bleed rate of the fresh grease. After $x/2b$=13.3 the oil bleed rate was 43.1% higher. For Grease 1 the same procedure was accomplished. The oil bleed rate changed 3.7% for $x/2b$=0.9 and 14.8% for $x/2b$=13.3. The damaged thickener of Grease 5 can help to lubricate the contact with base oil, which can temporarily reduce wear. Since the squeezed out base oil cannot stay in position, new problems occur. Furthermore, the grease life will be decreased. The grease contains solid lubricants which might aid the wear reduction, however no clear indication of this was seen. All results can be seen in Table 8.

7. Discussion

Fig. 23 graphically compares the properties of the greases in relation to Grease 1, which is set as reference. The absolute values are given in Table 2. Even though all greases are used in the application, they show vastly different properties. The base oil viscosity at 40 °C for example varies between 13 and 420 mm^2/s. Furthermore, the base oil types, thickeners, additives, and additional solid lubricants differ.

Fig. 24. graphically compares the experimental results of all greases in relation to Grease 1. The absolute values and standard deviations are given in Table 9.

Comparing the damage ratio using the maximum roughness values to exclude polishing effects of wear, variations between 2.37 (Grease 4) and 5.83 (Grease 5) in the $x/2b$=0.9 experiments were found. Three greases showed better behaviour than the reference. Furthermore, for $x/2b$=13.3 only one of these greases shows better behaviour than the reference grease. The maximum damage ratios show variation from 2.68 (Grease 4) and 14.37 (Grease 3). Grease 4 with the lowest base oil viscosity (13 mm^2/s) and highest oil bleed rate (11,9%) shows the best performance in the damage ratio. Low base oil viscosities lead to a better re-flow behaviour. The high oil bleed rate supplies the contact zone with more base oil. This positive effect may change in a real pitch bearing with increasing cycles as the grease life may decrease due to the high bleeding rate.

With a few exceptions, the SRV-tests showed similar results for the grease lubricants. For the greases 1, 4, 5, and 6 the mean diameter was between 0.31 mm and 0.37 mm for both tested conditions. Harsh wear was found for grease 2 (0.56 mm and 0.48 mm) and grease 3 (test

did not run till the end due to high wear). The viscosities of grease 2 (295 mm^2/s) and grease 3 (420 mm^2/s) are comparatively high. The results under pure sliding are in good agreement with $x/2b$=13.3 bearing tests and are partly in line with the observations of Maruyama et al. [49]. For small oscillations grease lubricants with low viscosities and high bleeding rates show better performance.

The comparison of the two test methods shows that assessments of the occurrence of wear can be made with model tests under pure sliding. Gravity, occurring wear debris, and the change of micro and macro geometry of the raceway have an influence in the bearing test. Therefore, the deviations for the results with different grease lubricants are much larger.

It must be kept in mind that the damage ratio, while being a quantitative parameter, alone is not an adequate parameter to evaluate the wear behaviour of the grease in the tribo-system. The reason being that wear may also cause a reduced surface roughness and thus a value suggesting improvement even with significant wear.

Another very important observation is that the mounting position of the bearing, i. e., the surrounding of the bearing, strongly influences the wear characteristics. This is due to the fact, that gravity, acceleration forces, and vibrations can have a detrimental or even positive effect on the redistribution of the grease causing the contacts to be starved respectively replenished. This of course needs to be considered when transferring experimental results to real applications, which often have very different environmental forces acting on the grease. This observation of course is even more important in combination with the consistency, i. e., NLGI class, and possibly the oscillating amplitude.

For the additional experiments with $x/2b$=29.1 no wear occurs for all grease lubricants. Due to the large oscillating amplitude it could be possible to reach hydrodynamic lubrication.

The lubricants contain additives and solid lubricants, which may influence the wear behaviour. No detailed information on the exact chemical composition are given by the manufactures, and the determination and publication of the exact chemical compositions is not the focus of the work. The influence of additives and tribolayers on wear behaviour in oscillating bearings are of great interest for further research.

It should be noted that no grease fully prevented wear in all operating conditions. However, some greases show promising behaviour in certain operating conditions, e. g., reference grease at small oscillating amplitudes. Thus a very careful understanding of the operating conditions is necessary to choose a lubricant. Furthermore, a change in the operating/surrounding conditions, e. g., change of pitch control behaviour in a wind turbine, may be a more effective method to limit wear. As shown in Stammler et al. the change of the controller concept can change the conditions of pitch bearings significantly [47].

Wind turbine pitch bearings use systems for relubrication. The chosen lubrication interval will also have a significant impact on the wear that occurs. In addition, it must be noted, that greases in wind turbine pitch bearings are often interact with corrosion protection, and cleaning agents (sometimes water-based), which also influence wear.

Finally it should be noted that in a tribological system the behaviour is governed by the interactions of all system components. Thus, a transfer to scaled experiments for an understanding of grease behaviour is useful and can be an important step to choose the correct lubricant for an application. However, care should always be taken when directly transferring laboratory experimental results to an application.

8. Conclusion

The behaviour of greases in downscaled oscillating bearing (7208) experiments and SRV tests was investigated. The focus was on three operating conditions, which were determined by analysing a multi-megawatt reference wind turbine. These operating conditions are characterised by the x/2b ratio, with ratios of 0.9, 13.3, and 29.1. Within the limits of the scaling methodology, the following conclusions could be shown.

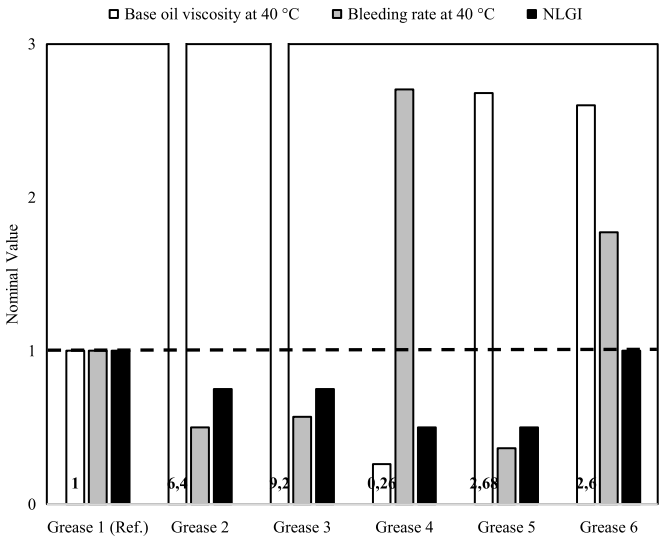

Fig. 23. Nominal grease properties.

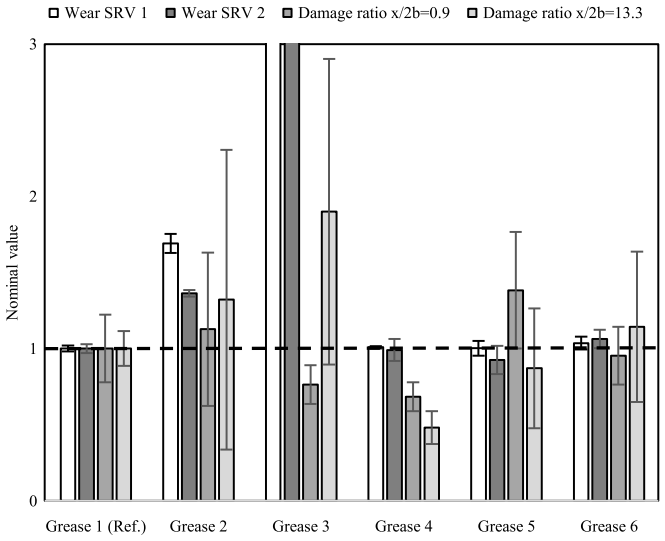

Fig. 24. Nominal results of grease investigations.

It could be shown that for small movements (x/2b=0.9) False Brinelling occurred for all tested grease lubricants. The smaller x/2b, the more often these conditions occurred in the reference system. Greases with low base oil viscosities and high bleeding rates showed the least wear, since the bleed oil can reflow in the contact zone.

For bigger movements (x/2b=13.3) severe wear occurred, which makes a comparison between the greases difficult. For large amplitudes (x/2b=29.1) no wear was visible.

It can be concluded, that the right grease needs to be tailored for the encountered operating conditions. Greases that perform well in some scenarios (e.g., small oscillating amplitudes) may well be detrimental in other conditions. So far, none of the investigated greases was able to show satisfactory wear protection in all the operating conditions encountered in wind turbine pitch bearings. Care should be taken when transferring experimental results to an application.

Table 9
Summary — grease lubricants under wind turbine pitch bearing conditions.

	Wear diameter		Mean Damage ratio SG		Max. Damage ratio SG	
	SRV1	SRV2	x/2b=0.9	x/2b=13.3	x/2b=0.9	x/2b=13.3
Grease 1	0.33 ± 0.006 mm	0.35 ± 0.010 mm	3.16 ± 0.70	4.55 ± 0,52	4.05	5.20
Grease 2	0.56 ± 0.020 mm	0.48 ± 0.008 mm	3.56 ± 1.59	6.01 ± 4.48	5.80	12.27
Grease 3	–[a]	–[a]	2.41 ± 0.40	8.64 ± 4.57	2.85	14.37
Grease 4	0.31 ± 0.003 mm	0.33 ± 0.025 mm	2.16 ± 0.30	2.19 ± 0.49	2.37	2.68
Grease 5	0.33 ± 0.032 mm	0.32 ± 0.033 mm	4.37 ± 1.21	3.96 ± 1,79	5.83	6.47
Grease 6	0.34 ± 0.014 mm	0.37 ± 0.021 mm	3.01 ± 0.60	5.20 ± 2.25	3.84	7.39

[a]SRV test does not run to the end due to high wear.

Nomenclature

α	Nominal contact angle
θ	Double oscillating amplitude
θ_r	Amplitude range
$\hat{\theta}$	Mean double oscillating amplitude
$\hat{\theta}_i$	Mean double oscillating amplitude of time step
Λ	Lambda ratio
μ	Coefficient of friction
μ_{Hertz}	Auxiliary coefficient Hertz
ν	Auxiliary coefficient Hertz
ρ	Calculated osculation
σ	Poisson's ratio
τ	Auxiliary angle Hertz
a	Half length of the contact area
A	Auxiliary coefficient Hertz
b	Half width of the contact area
B	Auxiliary coefficient Hertz
d	Inner bearing diameter
D	Outer bearing diameter
D_{P}	Rolling diameter
$D_{\text{P,O}}$	Contact point between roller and raceway
D_{WK}	Roller diameter
f	Oscillation frequency
f_{i}	Mean oscillation frequency of time step
F_{N}	Normal load
h_{min}	Minimum film thickness
i	Time step
M_{x}	Bending Moment
M_{y}	Bending Moment
N	Cycle
P	Contact pressure
P_i	Mean contact pressure of time step
Q	Roller load
R_{a1}	Roughness of contact 1
R_{a2}	Roughness of contact 2
SG	Damage ratio
Sz_{EXP}	Surface roughness after experiment
Sz_{NEW}	Surface roughness of new specimen
v_{max}	Maximum roller velocity
V	$(1-2\sigma^2)$
x	Distance covered by rolling element

CRediT authorship contribution statement

Fabian Schwack: Idea, theoretical and experimental work, writing. **Norbert Bader:** Data curation, writing. **Johan Leckner:** Model experiments, Data curation, writing. **Claire Demaille:** Model experiments. **Gerhard Poll:** Supervision.

Declaration of competing interest

The authors declare that they have no known competing financial interests or personal relationships that could have appeared to influence the work reported in this paper.

Acknowledgements

The authors would like to thank the German Federal Ministry for Economy Affairs and Energy (BMWi) for funding the project Highly Accelerated Pitch Bearing Test (HAPT — Project number 0325918) from which this paper originated. The simulation results presented here were partially carried out on the cluster system at the Leibniz University of Hannover, Germany. Furthermore the authors would like to thank Felix Prigge, Sirin Gnadeberg, Artjom Byckov, Steffen Helmedag and Fabian Halmos for supporting the presented research.

References

[1] A. Palmgren, Die Lebensdauer von Kugellagern, Zeitschrift Vereines Deutscher Ingenieure 68 (4) (1924) 339–341.
[2] G. Lundberg, A. Palmgren, Dynamic capacity of roller bearing, Acta Polytech. Mech. Eng. Ser. 1 (3) (1947) 1–52.
[3] A. Palmgren, Neue Untersuchungen über Energieverluste in Wälzlagern, Grundlagen der Wälzagertechnik (1957).
[4] B.J. Hamrock, D. Dowson, Isothermal elastohydrodynamic lubrication of point contacts: Part 1 – Theoretical formulation, J. Lubr. Technol. 98 (2) (1976) 223–228.
[5] B.J. Hamrock, D. Dowson, Isothermal elastohydrodynamic lubrication of point contacts: Part 2 – Ellipticity parameter results, J. Lubr. Technol. 98 (3) (1976) 375–381.
[6] B.J. Hamrock, D. Dowson, Isothermal elastohydrodynamic lubrication of point contacts: Part 3 – Fully flooded results, J. Lubr. Technol. 99 (2) (1977) 264–275.
[7] F. Schwack, M. Stammler, G. Poll, A. Reuter, Comparison of life calculations for oscillating bearings considering individual pitch control in wind turbines, J. Phys. Conf. Ser. 753 (2016) 112013.
[8] M. Stammler, F. Schwack, N. Bader, A. Reuter, G. Poll, Friction torque of wind-turbine pitch bearings – comparison of experimental results with available models, Wind Energy Sci. 3 (1) (2018) 97–105.
[9] T. Maruyama, T. Saitoh, Oil film behavior under minute vibrating conditions in EHL point contacts, Tribol. Int. 43 (8) (2010) 1279–1286.
[10] M.O.L. Hansen, Aerodynamics of Wind Turbines, third ed., Routledge, 2015.
[11] J. Zhang, M. Cheng, Z. Chen, X. Fu, Pitch angle control for variable speed wind turbines, Electr. Util. Deregul. Restruct. Power Technol. (2008) 2691–2696.
[12] K. Fischer, F. Besnard, L. Bertling, Reliability-centered maintenance for wind turbines based on statistical analysis and practical experience, IEEE Trans. Energy Convers. 27 (1) (2012) 184–195.
[13] M. Stammler, J. Wenske, Integration von schadensmechanismusanalyse und blattlagertests in den entwicklungsprozess von WKA, VDI-Fachtagung Gleit- und Wälzlagerungen (2015).
[14] T. Burton, D. Sharpe, N. Jenkins, E. Bossanyi, Wind Energy Handbook, second ed., Wiley & Sons, London, 2012.
[15] E.A. Bossanyi, Individual blade pitch control for load reduction, Wind Energy 6 (2) (2003) 119–128.
[16] E.A. Bossanyi, Further load reductions with individual pitch control, Wind Energy 8 (4) (2005) 481–485.
[17] R. Karbacher, Fettschmierung von Wälzlagern bei oszillierender Beanspruchung, Tribol. Schmierungstech. 45 (5) (1998) 23–31.
[18] M. Grebe, P. Feinle, W. Hunsicker, Möglichkeiten zur Reduzierung von False Brinelling Schäden, in: Reibung, Schmierung Und Verschleiss, in: Reibung, Schmierung und Verschleiß, GfT, Aachen, 2008.
[19] T. Maruyama, T. Saitou, A. Yokouchi, Differences in mechanisms for fretting wear reduction between oil and grease lubrication, Tribol. Trans. 60 (3) (2016) 497–505.
[20] C. Schadow, Stillstehende fettgeschmierte Wälzlager unter dynamischer Beanspruchung (Doctoral-Thesis), Otto-von-Guericke-Universität, Magdeburg, 2016.
[21] M. Grebe, P. Feinle, Brinelling, false-brinelling, false false-brinelling, in: Reibung, Schmierung Und Verschleiss, GfT, Aachen, 2006.

[22] D. Godfrey, Fretting corrosion or false brinelling?, Tribol. Lubr. Technol. 59 (12) (2003) 28–29.
[23] R. Errichello, Another perspective: False brinelling and fretting corrosion, Tribol. Lubr. Technol. 60 (4) (2004) 34–36.
[24] D. Godfrey, Iron oxides and rust (hydrated iron oxides), Lubr. Eng. 1999 (2) (1999) 33–37.
[25] H.R. Hertz, Über die Berührung fester elastischer Körper, J. Reine Angew. Math. 92 (1881) 156–171.
[26] D. Godfrey, A study of fretting wear in mineral oil, Lubr. Eng. 12 (1) (1956) 37–42.
[27] F. Schwack, A. Byckov, N. Bader, G. Poll, Time-dependent analyses of wear in oscillating bearing applications, in: STLE 72th Annual Meeting and Exhibition, 2017.
[28] M. Stammler, A. Reuter, G. Poll, Cycle counting of roller bearing oscillations – case study of wind turbine individual pitching system, Renew. Energy Focus 25 (2018) 40–47.
[29] W. Popko, P. Thomas, A. Sevinc, M. Rosemeier, M. Bätge, R. Braun, F. Meng, D. Horte, C. Balzani, O. Bleich, et al., IWES Wind Turbine IWT-7.5-164, Rev.4 (2018).
[30] J. Jonkman, S. Butterfield, W. Musial, G. Scott, Definition of a 5-MW Reference Wind Turbine for Offshore System Development, National Renewable Energy Laboratory, Golden, CO, Technical Report No. NREL/TP-500-38060, 2009.
[31] C. Bak, F. Zahle, R. Britsche, T. Kim, A. Yde, L.C. Henriksen, M.H. Hansen, J.P. Blasques, M. Gaunaa, A. Natarajan, The DTU 10-MW Reference Wind Turbine, Danish Wind Power Research, Technical University of Denmark, Denmark, 2013.
[32] International Electrotechnical Commission, IEC 61400-1 edition 3 – wind turbines – Part 1: Design requirements, 2005.
[33] F. Schwack, M. Stammler, H. Flory, G. Poll, Free contact angles in pitch bearings and their impact on contact and stress conditions, Eur. Wind Energy Assoc. (2016).
[34] M.N. Kotzalas, G.L. Doll, Tribological advancements for reliable wind turbine performance, Philos. Trans. R. Soc. Lond. Ser. A Math. Phys. Eng. Sci. 368 (1929) (2010) 4829–4850.
[35] G. Chen, J. Wen, Load performance of large-scale rolling bearings with supporting structure in wind turbines, J. Tribol. 134 (2012).
[36] M. Stammler, S. Baust, A. Reuter, G. Poll, Load distribution in a roller-type rotor blade bearing, J. Phys. Conf. Ser. 1037 (2018) 042016.
[37] D. Becker, Hoch belastete Großwälzlagerungen in Windenergieanlagen, Vol.16, (Doctoral-Thesis), Shaker, Aachen, 2012.
[38] Y. Wang, Q. Yuan, Static load-carrying capacity and fatigue life of a double row pitch bearing with radial interference, Proc. Inst. Mech. Eng. C 228 (2) (2013) 307–316.
[39] R. Liu, H. Wang, B.T. Pang, X.H. Gao, H.Y. Zong, Load distribution calculation of a four-point-contact slewing bearing and its experimental verification, Exp. Tech. 42 (3) (2018) 243–252.
[40] F. Massi, J. Rocchi, A. Culla, Y. Berthier, Coupling system dynamics and contact behaviour: Modelling bearings subjected to environmental induced vibrations and 'false brinelling' degradation, Mech. Syst. Signal Process. 24 (4) (2010) 1068–1080.
[41] D. Tonazzi, F. Massi, Lt Baillet, J. Brunetti, Y. Berthier, Interaction between contact behaviour and vibrational response for dry contact system, Mech. Syst. Signal Process. 110 (2018) 110–121.
[42] J. Aguirrebeitia, R. Avilés, I. Fernández de Bustos, M. Abasolo, Calculation of general static load-carrying capacity for the design of four-contact-point slewing bearings, J. Mech. Des. 132 (6) (2010) 064501.
[43] J. Aguirrebeitia, M. Abasolo, R. Avilés, I. Fernández de Bustos, General static load-carrying capacity for the design and selection of four contact point slewing bearings: Finite element calculations and theoretical model validation, Finite Elem. Anal. Des. 55 (2012) 23–30.
[44] J. Aguirrebeitia, M. Abasolo, R. Avilés, I. Fernández de Bustos, Theoretical calculation of general static load-carrying capacity for the design and selection of three row roller slewing bearings, Mech. Mach. Theory 48 (2012) 52–61.
[45] J. Aguirrebeitia, J. Plaza, M. Abasolo, J. Vallejo, Effect of the preload in the general static load-carrying capacity of four-contact-point slewing bearings for wind turbine generators: Theoretical model and finite element calculations, Wind Energy 17 (10) (2014) 1605–1621.
[46] A. Daidie, Z. Chaib, A. Ghosn, 3D simplified finite elements analysis of load and contact angle in a slewing ball bearing, ASLE Trans. 130 (8) (2008).
[47] M. Stammler, P. Thomas, A. Reuter, F. Schwack, G. Poll, Effect of load reduction mechanisms on loads and blade bearing movements of wind turbines, Wind Energy 23 (2) (2019) 274–290.
[48] P.M. Lugt, Grease Lubrication in Rolling Bearings: Tribology Series, first ed., John Wiley & Sons, Chichester, 2013.
[49] T. Maruyama, T. Saitoh, A. Yokouchi, Differences in mechanisms for fretting wear reduction between oil and grease lubrication, Tribol. Trans. 60 (3) (2017) 497–505.
[50] Deutsches Institut für Normung, DIN 51834 - Testing of lubricants - Tribological test in the translatory oscillation apparatus, Beuth Verlag (2010).
[51] Deutsches Institut für Normung, DIN 51817 - Testing of lubricants - Determination of oil seperation from greases under static conditions, Beuth Verlag (2010).
[52] Deutsches Institut für Normung, DIN ISO 2137 - Petroleum products and lubricants - Determination of cone penetration of lubricating greases and petrolatum, Beuth Verlag (2016).
[53] ASTM Iternational, ASTM D6595-17 - Standard Test Method for Determination of Wear Metals and Contaminants in Used Lubricating Oils or Used Hydraulic Fluids by Rotating Disc Electrode Atomic Emission Spectrometry, West Conshohocken (2017).
[54] F. Schwack, F. Prigge, G. Poll, Finite element simulation and experimental analysis of false brinelling and fretting corrosion, Tribol. Int. 126 (2018) 352–362.
[55] H.L. Heathcote, The ball bearing: In the making, under test and on service, Proc. Inst. Automob. Eng. 1 (15) (1920) 569–702.
[56] M. Grebe, False Brinelling - Standstill Marks at Roller Bearings, (Doctoral-Thesis), Slovak University of Technology, Bratislava, 2012.